Acta Polytechnica **64**(6):588–604, 2024
https://doi.org/10.14311/AP.2024.64.0588

Published by the Czech Technical University in Prague

SETTLEMENT OF PILES WITH NEGATIVE SKIN FRICTION: DESIGN APPROACHES ACCORDING TO PART 3 OF EUROCODE 7

Alena Zemanová*, Vojtěch Anderle, Jan Masopust

Czech Technical University in Prague, Faculty of Civil Engineering, Department of Geotechnics, Thákurova 7, 166 29 Prague, Czech Republic

* corresponding author: alena.zemanova@fsv.cvut.cz

Abstract. Piles offer an effective solution for supporting structures in challenging ground conditions. However, ground settlement around deep foundations can induce negative skin friction, adding complexity to the geotechnical analysis and requiring careful consideration in both the pile settlement evaluation and structural integrity design. The article discusses the general recommendations provided by the informative annex of the revised Eurocode 7 version for designing piles subjected to negative skin friction. Using the Fellenius unified pile design concept, we provide a practical design framework for piles subjected to negative skin friction that extends the load-settlement curve methods proposed by Masopust, representing the standard pile design approaches in the Czech Republic. For examples presented, the introduced practical approach, also suitable for manual calculations, is in very good agreement with a refined calculation providing a nonlinear load-settlement curve.

Keywords: Negative skin friction, load-settlement curves, pile settlement, pile design, soil settlement, Eurocode 7.

1. Introduction

1.1. Motivation

Piles can be a very effective way to provide foundations for structures. These deep foundations are used in various situations, such as high-rise buildings, bridges, or offshore structures [1–5].

Negative skin friction is a phenomenon that can occur when the soil surrounding the pile shaft settles more than the pile itself. Soil settlement around piles can occur for a variety of reasons, including consolidation of soft soil layers, settlement due to embankment surcharge caused by ground elevation or other loading of adjacent structures, groundwater lowering, cyclic loading, or earthquakes [6]. The pile foundation of a bridge abutment can be a typical example of a transport construction, where negative skin friction can occur after backfilling behind the retaining structure and subsequent consolidation settlement of the deeper soft soil layers. Soil settlement reduces the positive shaft resistance or may even cause downward drag and increase the pile loading (with negative skin friction force called drag force). Thus, the pile is subjected to an additional settlement, or the increase in force may even result in its structural failure.

The response of individual piles can be determined by load tests or alternatively calculated using empirical, analytical approaches, or numerical simulations. If negative skin friction significantly affects pile response, it must be properly reflected in the pile design. For this reason, any (preliminary) calculation method should be able to consider these effects.

1.2. Literature review

The discussion on negative skin friction and its consideration in pile design has been underway in the professional community of researchers and geotechnical engineers for several decades. Thus, a significant number of investigations regarding negative skin friction have been carried out over the past few decades.

Early work on this topic focused on full-scale field tests and experimental measurements of pile settlement and load distribution in driven steel pipe or concrete piles [7–11], and also for bitumen-coated piles and pile groups [12–17]. These were followed by a series of centrifuge model studies [18–22] or small-scale model tests [16, 23], and more recently large-scale experiments [24].

Analytical approaches using a closed-form solution [12, 25] have been developed in parallel based on the experimental findings. These simplified methods often empirically estimate the position of the *neutral point* or *neutral plane*, where the negative skin friction switches to positive shaft resistance, and further determine the drag force assuming fully mobilised negative skin friction regardless of the magnitude of the soil settlement. The existing simplified solutions usually overestimate the depth of the neutral plane and thus can be considered as an upper limit of the response [24, 26].

In contrast to previous studies, Fellenius suggested that the negative skin friction problem is a pile settlement issue rather than an ultimate geotechnical capacity issue and introduced his *unified pile design concept* accounting for negative skin friction in a pile settlement analysis [27]. His iterative scheme involves balancing the forces acting on the pile and the set-

tlement of the pile and soil simultaneously, as they are related and cannot be considered separately. This approach, later generalised to pile groups [6, 28], is one of the most widely used simplified methods for estimating negative skin friction.

Later, continuum approaches were proposed for homogeneous soil [29], based on the theory of homogeneous elastic half-space, employing Mindlin's solution [30] and later modified for a layered soil deposit [31] using a mean modulus. This analytical model was verified against finite element analyses from the literature, and a practical procedure was proposed using a parametric dimensionless solution [31]. Poulos also introduced an *approximate hand method* for piles subjected to axial load and negative skin friction [32, 33]. Unlike Fellenius, he does not iteratively search the neutral plane but sets it at the depth of the soil movements. This plane divides the ground profile into consolidating and stable zones and designs a sufficient pile length to meet the design requirements, causing structural capacity and pile settlement to be affected by negative skin friction. His conservative approach provides meaningful predictions of pile behaviour (compared to a boundary element solution) for piles subjected to relatively large soil settlements.

The load-transfer method [34] has gradually become a popular tool in pile design [35–41] widely accepted in practice [42, 43]. This approach requires stress transfer functions derived from field or laboratory tests describing shear stresses acting on the pile shaft as a function of the pile settlement. A hyperbolic law is often assumed to govern the pile-soil interface behaviour [37, 44, 45]. Wong et al. proposed a load-transfer model using hyperbolic soil springs for the pile-soil interface to address the behaviour of piles under negative skin friction in stratified soil deposits and established a procedure for evaluating the input parameters from conventional soil tests [37]. In general, the load transfer method framework provides a suitable framework for analysing the nonlinear pile settlement and also for performing inverse analyses, e.g., [37, 42, 46]. In addition, the effect of the negative skin friction time-dependency due to the nonlinear soil consolidation and loading–unloading conditions can be taken into account, such as in an improved hyperbolic model using the load transfer method for the pile–soil interface in [45].

Numerical methods, often used to verify other approaches, complete the list of computational methods able to capture the increasing number of factors related to soil-pile interaction and negative skin friction [17, 23, 26, 47–51]. The importance of properly modelling the soil-pile interaction was demonstrated in [48] using both the no-slip and slip analyses for the prediction of the dragload development. In this elastoplastic finite element analysis, an isotropic elastic model represented single piles and piles in groups, whereas a non-associated Mohr-Coulomb model was used for soils. Unlike the slip analysis using interface elements, the conventional no-slip continuum analysis predicted unrealistic responses in which the dragloads were substantially overestimated. As shown in a study focused on the dragload group effect for pile groups [26], the finite difference method with interface elements can be used equally successfully for the numerical modelling of pile groups under negative skin friction. Another detailed simulation using geotechnical software coupled with programs for structural analysis was introduced in [49] to analyse the response of buildings with pile foundations to a tunnel construction, where the ground surface settlements may also induce negative skin friction on the pile shaft. Recently, more and more advanced numerical models have been developed, such as the elasto-viscoplastic model taking into account the effect of soil creep [51].

As seen from the above overview, many sophisticated approaches were introduced. However, they are often too complicated and time-consuming for practical use and require a significant amount of input data, which are often not available and must be estimated.

1.3. Negative skin friction in current European standards

The recommendations in design standards, including the European standards for geotechnical structures Eurocode 7 (EC7), have gradually evolved based on the developments in the field.

EC7 [52] aimed to bridge a gap between an explicit and codified approach for the upper structure above the ground level and simple or empirical calculations for the underlying geotechnical substructures based on highly subjective assessments of design properties [53]. Nevertheless, the first version of EC7 contains only a few very general recommendations for designing piles subjected to negative skin friction and does not give detailed instructions or examples for its consideration [54].

However, the second generation of EC7, which is currently in the approval process, extends the design guidelines on assessing negative skin friction in one of its informative annexes in the third part of the standard prEN 1997-3: Annex C.9 Downdrag due to vertical ground movements [43]. Outlines of a rigorous interaction model and simplified approaches for the downdrag consideration are briefly introduced in the annex. Let us summarise its key points:

- The possible adverse effect of negative skin friction shall be included in both limit states – always in the serviceability limit state and for the drag force higher than any variable compressive forces applied to the pile also in the ultimate limit state.
- A ground-pile interaction analysis shall provide the depth of the *neutral plane* (the boundary between negative and positive friction and the point of the equality of the ground and pile settlement) complemented with force and displacement distributions. Note that the position of the neutral plane differs for both limit states.

- The drag force, classified as permanent action, results from negative skin friction forced by reverse relative soil-pile movement – downdrag. A cautious drag force estimate should be derived from the upper values of the ground properties.

It is clear from the above points that the forthcoming version of the European standard EC7 deals with the negative skin friction for both limit states. As mentioned in the literature review, Fellenius suggested that negative skin friction design should be aimed at pile settlement [27]. Concerning the ultimate limit state, higher axial force due to the negative skin friction should be examined as the structural integrity of the pile itself may be affected [32] whereas the ultimate geotechnical axial load capacity of a pile is not affected by the negative skin friction (unless a strain-softening at the pile/soil interface occurs [33]).

The rigorous interaction model is schematically shown in Figure 1. The ground settlement s_{soil}, including the immediate, primary, and possibly secondary consolidation, should consider changes in effective stresses, ground stiffness, and the depth of the compressible ground. For pile settlement s_{pile}, any analytical, empirical, numerical, or other approach can be used, taking into account the stress distribution. It is pointed out that the pile and ground settlement and the neutral point can be found from the interaction analysis. If the compressive forces are combined in both limit states, then either the drag force or the leading variable action should be considered.

For specific cases, the guidance provides the following simplified approaches:

- For serviceability limit state, the base of the consolidating soil layer can be assumed as the neutral plane, and the drag force corresponds to the full depth of the settling soil layer.
- For ultimate limit state, the base of the consolidating soil layer can be considered as the neutral plane if the pile settlement is much smaller than the settlement of the surrounding ground. If the pile settlement is greater than that of the surrounding soil, the neutral point can be located at the ground surface, and the drag force may be disregarded.

1.4. Goal of the study

This study aims to show how negative skin friction can be incorporated into standard pile design methods. The new Part 3 of EC7 (prEN 1997-3) recommendations motivated the approaches presented in this paper. We provide a simple framework for designing piles subjected to negative skin friction extending the load-settlement curve methods proposed by Masopust [55–59]. We limit our attention to the serviceability limit state as it is very likely to be the decisive state for the design of large-diameter boring piles in soft soils with its base in soils or weak rocks, which are the subject of interest of this study.

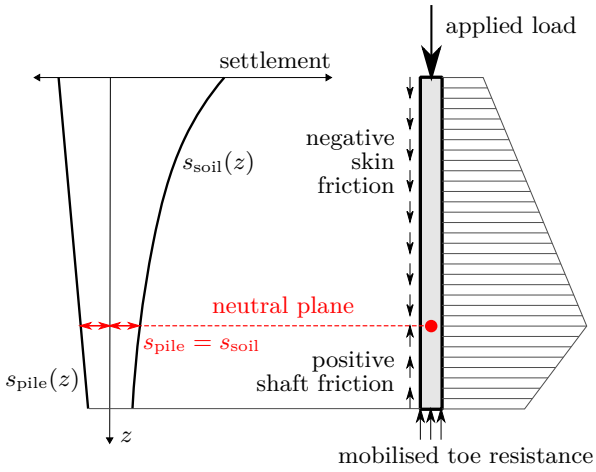

Figure 1. Settlement and force distribution.

2. Methods for pile-settlement and negative skin friction consideration

Practical approaches for pile settlement design are often based on the load-settlement curve method or use load transfer functions [43]. The design methods proposed by Masopust [55–58] belong to the group of engineering approaches focusing on the design of axially-loaded bored piles. Approximately 350 static load tests performed on bored single piles in the Czech Republic and partially in Germany provided the dataset for back analysis of pile responses in different soil deposits. These field test results allowed to establish a quadratic-linear approximation of the load-settlement curve, useful for manual calculations, and a computing procedure providing a nonlinear load-settlement curve. Both approaches, used for practical pile design for decades, consider the effect of the pile installation, i.e. pile drilling, borehole cleaning, method of concreting, and shaft insulation, on the bearing capacity of the pile.

2.1. Quadratic-linear load-settlement curve approximation

The first method is based on the Poulos practical model for load-settlement analysis of piles [31, 58]. Likewise, in the original approach, the construction of the load-settlement curve is simplified to the determination of two points, corresponding to the full mobilisation of skin friction $(s_{\text{y}}, R_{\text{y}})$ and 25 mm settlement (s_{25}, R_{25}). However, compared to the original procedure, the first part of the load-settlement curve, before the point $(s_{\text{y}}, R_{\text{y}})$, was replaced by a parabola (Figure 2), and the method was modified using the measured responses and their back analysis for the predictions of the shaft and base resistance. Detailed instructions for the construction of the load-settlement curve can be found in Appendix A.1 and also in the Czech standard ČSN 731004 Geotechnical Design – Foundations – Requirements for calculation methods [59]. According to those documents, the shaft

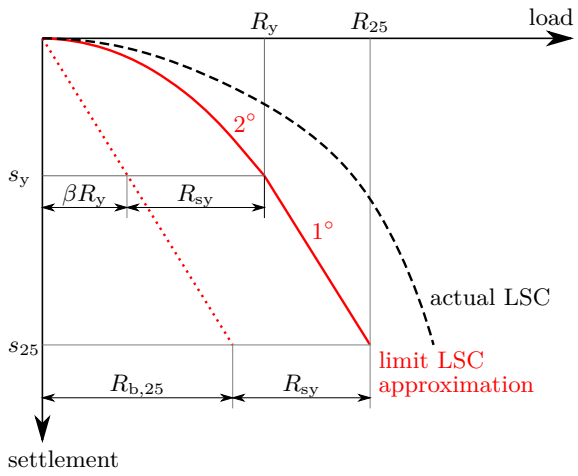

FIGURE 2. Load-settlement curve (LSC) approximation.

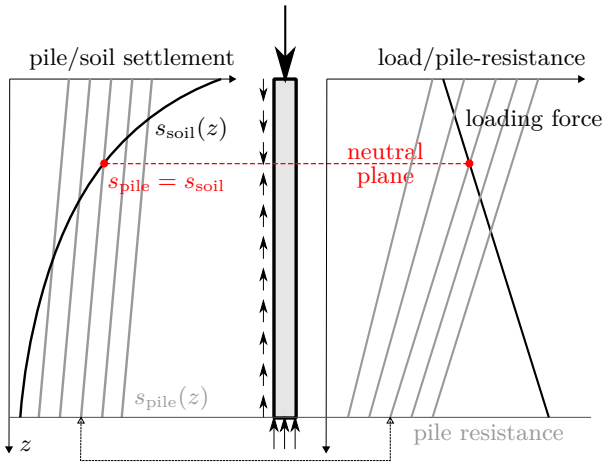

FIGURE 4. Equilibrium of settlements and forces.

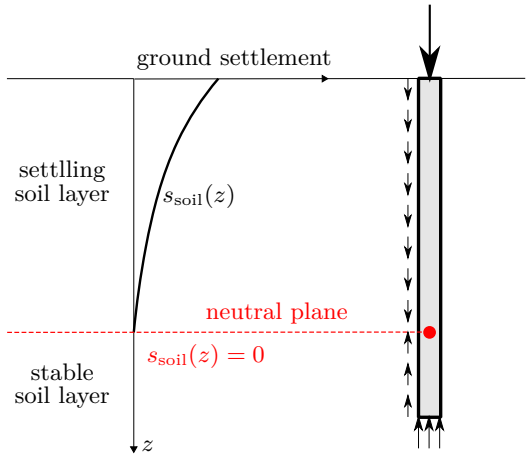

FIGURE 3. Pile in settling and stable zone.

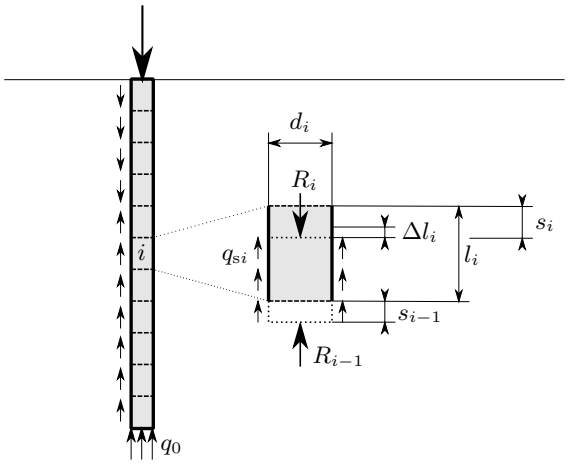

FIGURE 5. Scheme of pile discretisation.

friction and base resistance values are then derived from the tabulated values of regression coefficients.

In terms of negative skin friction incorporation, this approximation method can be combined with the simplified approach mentioned in EC7, i.e. as far as a boundary between less compressible *stable soil* and softer *settling soil* can be estimated, this boundary is conservatively considered the neutral plane (Figure 3). Then, the drag force can be determined in the settling zone under the assumption that the full mobilisation of the negative skin friction occurred [33]. However, some studies suggest reducing the negative skin friction compared to its positive values, and a degree of mobilisation corresponding to a factor of 0.67 can be found in the literature [27]. Also, the Czech national standard ČSN 731004 [59] notes that the negative friction can be estimated as 70 % of the positive shaft friction.

Alternatively, the depth of the neutral plane can be estimated with more detailed procedures described in [27, 32]. For our comparative study, we used the Fellenuis *unified pile design concept* [27] combined with the semi-empirical load-settlement curve approximation from [58]. A set of pile-settlement plots and corresponding load distribution curves (starting from the base resistance and increasing with the positive shaft resistance) is constructed. Then, the location of the neutral plane is found iteratively to achieve both the load/resistance and pile/soil settlement equilibrium in the system (Figure 4). Finally, the pile settlement corresponding to this point is supposed to be the resultant one.

2.2. Procedure providing nonlinear load-settlement curve

In the nonlinear approach, the pile is divided into a few segments (Figure 5). A sequence of small, gradual growing vertical displacements (settlements s_0) is given to the pile base, and the corresponding pile base resistance q_0 is evaluated. Then, the shaft frictions q_{si}, axial forces acting on the bottom and top cross-section R_{i-1} and R_i, elastic contractions of the pile elements Δl_i, and settlements at the top of element s_i are determined subsequently from the pile base up to the pile head [31, 34, 55, 58].

This procedure provides settlement of the pile head with the corresponding pile load force and allows the construction of the nonlinear load-settlement curve.

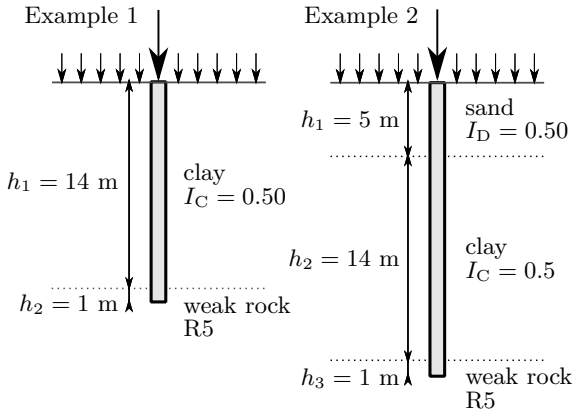

Figure 6. Scheme of analysed piles in stratified soil and weak rock deposits containing compressible clay.

The mobilised skin frictions q_{si} and pile base resistances q_0 are related to the pile movements by relationships derived, again, from the back-analyses of the static loading tests and summarised in Appendix A.2.

The relative pile/soil displacements are evaluated and used in the friction-settlements relationships if the surrounding soil settles. Thus, a nonlinear stress load-settlement curve reflecting the negative skin friction can be produced straightforwardly. Then, the increased pile settlement caused by the drag force can be directly retrieved from the shifted curve.

3. Examples

To show the effect of negative skin friction on pile settlement, we analyse the responses of two piles passing through a thick layer of soft to medium stiff clay with consistency index $I_C = 0.5$ (Figure 6). In both examples, the pile base is located in a weak rock R5 (compressive strength 1.5–5 MPa), and for the 20 m long pile, the clay layer is covered by a medium-dense sand layer ($I_D = 0.5$).

The lengths of the bored piles are 15 m and 20 m, with the diameter of the pile shaft of 0.8 m. Both concrete piles are subjected to a vertical force, while the soil surrounding the pile is further subjected to a surface load of 100 kPa, corresponding to an embankment approximately 5 m high. This additional surcharge causes soil settlement determined according to the Czech standard [59] using the oedometric moduli and unit weights listed in Table 1.

4. Results and discussion

From the problems outlined above, it is clear that the simplified approach mentioned in EC7 would predict enormous pile settlements in these cases because the stable soil layer surrounding the lower part of the piles is only 1 m thick. Such a low neutral plane position, close to the pile base, is very conservative and would significantly increase the force acting on the pile. The pile geometry would need to be re-designed due to the unacceptable settlement [60].

Parameter	Unit	Ex. 1	Ex. 2
Loading force $\overline{R}$	[kN]	1 600	1 900
Surcharge	[kPa]	100	100
Bored concrete pile			
Elastic modulus	[GPa]	30	30
Sand $I_D = 0.5$			
Unit weight	[kN m^{-3}]	-	19
Oed. modulus	[MPa]	-	41
Clay $I_C = 0.5$			
Unit weight	[kN m^{-3}]	20	20
Oed. modulus	[MPa]	32	32
Weak rock R5			
Unit weight	[kN m^{-3}]	21	21
Oed. modulus	[MPa]	120	120

Table 1. Loading and material properties.

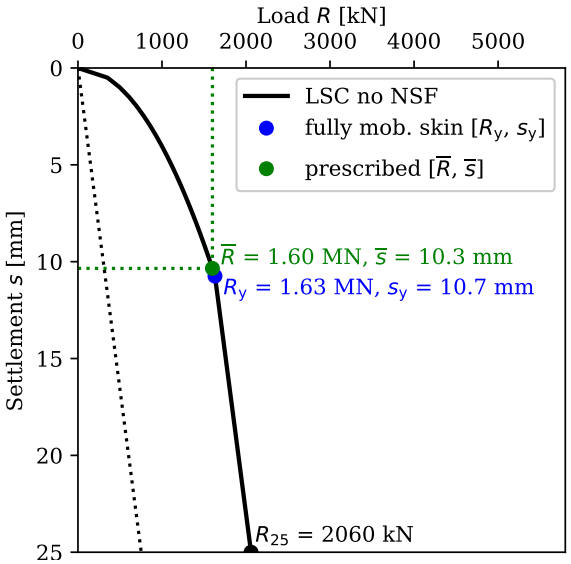

Figure 7. Example 1 – Quadratic-linear load-settlement curve (LSC) unaffected by negative skin friction (NSF) [59]; (colour online).

For this reason, let us present a more detailed model dealing with pile load-settlement curves, providing better predictions for the neutral plane positions. Appendix A includes additional data to reproduce the results presented. Furthermore, a GitLab repository was also created [61] containing the source codes for the graphs in Section 4.

4.1. Example 1

The values of the vertical forces acting on the pile heads are chosen so that the pile settlements without the negative skin friction were around 10 mm (Figure 7). Thus, the quadratic-linear approximation of the load-settlement curve for the 15 m long pile predicts a 10.3 mm settlement corresponding to the 1 600 kN vertical load, i.e. just above the point corresponding to the full mobilisation of skin friction.

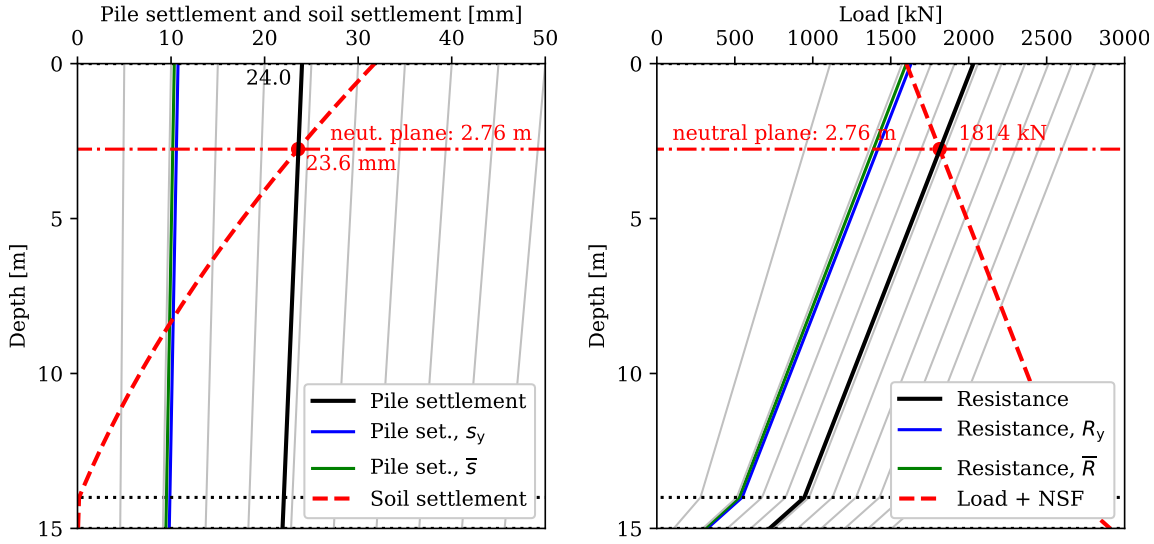

(A). Settlement. (B). Force evolutions.

FIGURE 8. Example 1 – Settlement and force evolutions including negative skin friction (NSF) effect along the pile length provided by the practical approach [59]; (colour online).

To determine the influence of the negative skin friction, settlement and force evolution curves (Figure 8) are constructed using the load-bearing capacities of the pile base and shaft according to the approximate method in Appendix A.1. Figure 8a shows the evolution of the pile settlement along its length compared to the soil settlement induced by the additional surface load. A set of pile settlements is constructed, assuming that the pile head settlement gradually increases from zero by 5 mm and the corresponding pile base settlement is simply estimated from the head settlement using the factor R_k representing the correction factor for pile compressibility, see [31] and Appendix A.1. The settlements corresponding to the prescribed load s_{user} and to the full mobilisation of skin friction s_y are highlighted. It is reasonable to assume that the settlement of the same pile affected by negative skin friction must be higher. The comparison with the soil settlement shows that even using the original pile settlement without the negative skin friction effects (10.3 mm) substantially increases the position of the neutral plane, from the original depth of 14 m below the level of the pile head to a depth of approximately 8 m.

Let us further refine the estimation of the neutral plane's position by balancing the equilibrium of the load force and the pile-bearing resistance on one side and the equality of settlement of the pile and the surrounding soil on the other. For this reason, the predictions of pile resistances corresponding to the previously retrieved pile settlements are determined (Figure 8b). For each value of the head settlement, the pile base resistance can be derived assuming that the relationship is linear with a known value of the base resistance at the shaft resistance activation (Appendix A.1). The pile bearing resistances gradually increase from the original pile base resistances at the level of the base towards the pile head due to the increasing pile shaft resistances calculated from the positive skin friction in individual soil layers. On the contrary, the loading force increases due to the drag load in the opposite direction, starting with the user-defined loading force at the pile head and ending with a maximum value at the pile base when the whole shaft is theoretically subjected to negative skin friction. The additional increase in the loading force acting on the pile due to the down drag is calculated from the negative skin friction derived from the fully mobilised positive one when the degree of mobilisation is assumed to be 0.7 [54, 59].

Finally, the neutral plane's position is found at the level where the soil-pile-settlement equality and load-resistance equilibrium coincide. For this example, this plane is located at a depth of 2.76 m measured from the pile head, and the pile head settlement corresponds to the value of 24 mm, i.e. it has more than doubled compared to its value without the negative skin friction effects.

The previous practical approach addressed how to account for negative skin friction when using the load-settlement semi-empirical approximation. The negative skin friction incorporation is more straightforward for the refined approach providing a nonlinear load-settlement curve. The only modification of the original procedure, presented in Appendix A.2, is that in calculating the mobilised skin friction, the pile settlement is replaced by its relative value, considering the surrounding soil vertical movement.

The comparison of both analyses is visualised in Figure 9. First, three load-settlement curves are compared (Figure 9a). The grey ones correspond to the quadratic-linear approximation and to the nonlinear

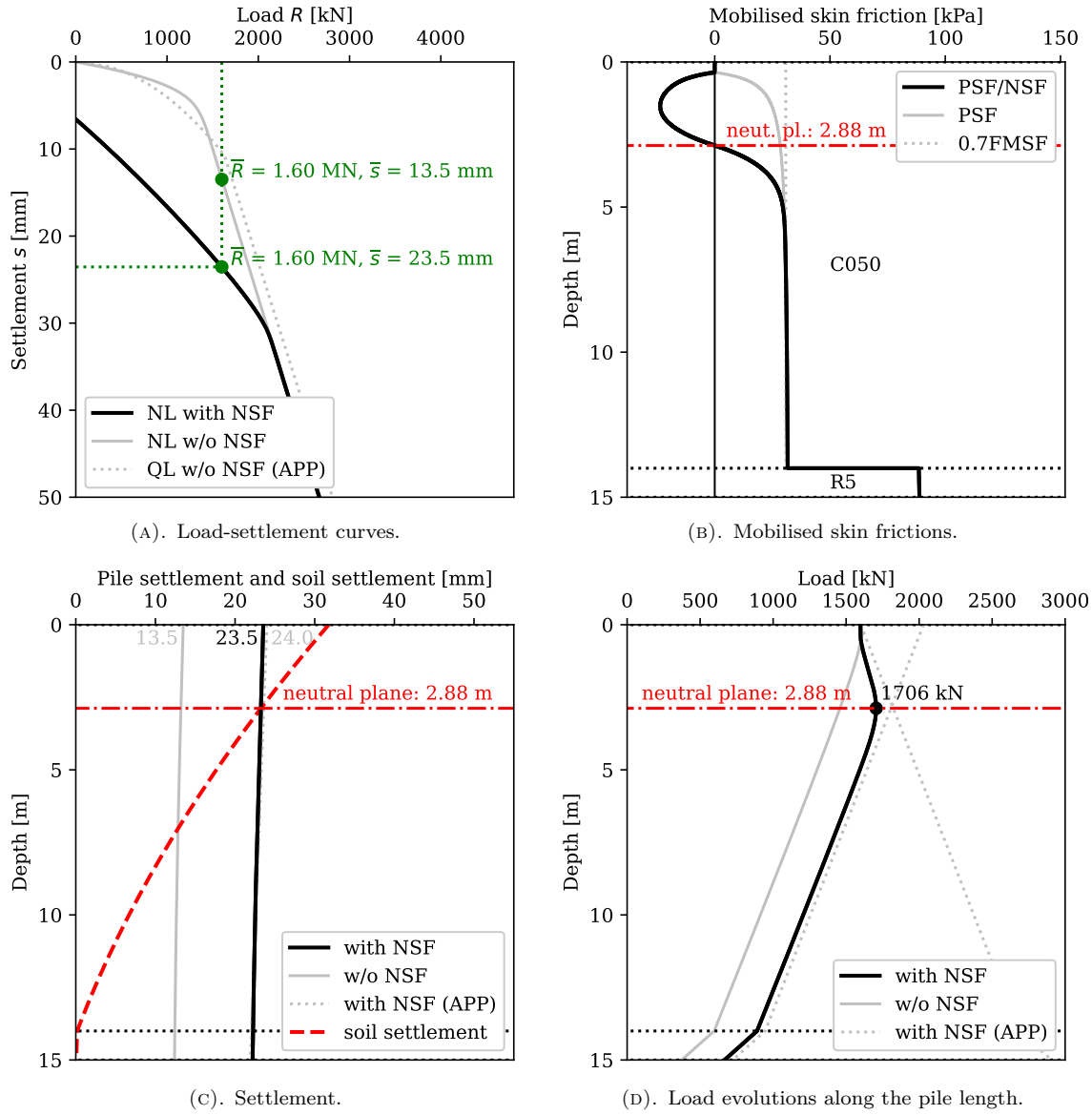

(A). Load-settlement curves.

(B). Mobilised skin frictions.

(C). Settlement.

(D). Load evolutions along the pile length.

Figure 9. Example 1 – Comparison of the load-settlement curves, mobilised skin frictions (negative (NSF), positive (PSF), or 70 % fully mobilised (0.7FMSF)), and settlement and load evolutions along the pile length by the refined nonlinear approach (NL) against the practical approximation (APP) using the quadratic-linear (QL) load-settlement curve; (colour online).

load-settlement curve unaffected by the negative skin friction. The black curve represents the pile behaviour considering the negative skin friction. This nonlinear curve is shifted because the pile settles due to the down drag even though a zero loading force is applied at the pile head.

In addition, the mobilised skin frictions are presented (Figure 9b). In the practical approximation, the limit shaft resistance is derived from the 70 % of the fully mobilised skin frictions, see Equation (4) in Appendix A.1, and we consider the same limit value for the negative skin friction. The refined approach determines the level of shaft friction based on the relative vertical movement of the pile and the adjacent soil. Thus, the shaft friction in the area around the neutral plane does not reach its limit value (Figure 9b). This reduced skin friction is then reflected in the evolution of the pile load-resistance curve along the pile length when the largest force action on the pile (Figure 9d) decreases from 1814 kN (predicted by the practical approach) to 1706 kN (predicted by the refined approach). Also, the lower negative skin friction results in a slightly smaller pile settlement; the practical approach provides a head settlement of 24 mm compared to the refined value of 23.5 mm (Figure 9c), which is on the safe side. If we compare the resulting position of the neutral plane, it remains almost unchanged for this example.

4.2. Example 2

The same analyses are repeated and performed for the second example, considering a longer pile passing through three layers of soil, where the layer of clay is additionally covered with a layer of sand (Figure 6).

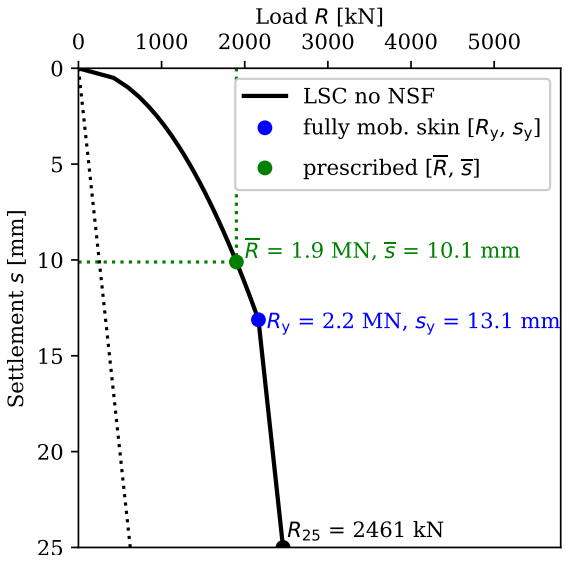

FIGURE 10. Example 2 – Quadratic-linear load-settlement curve unaffected by negative skin friction [59]; (colour online).

First, the behaviour of the pile without the influence of the surrounding ground settlement is analysed, and the resulting load-settlement curve is shown in Figure 10. In this case, the loading forces transferred from the upper structure to the pile would cause a settlement of approximately 10 mm, again, above the point of the full mobilisation of skin friction.

To derive the position of the neutral plane, the resulting settlement, and loading force, including the drag force, it is again necessary for the practical approach to construct a set of curves corresponding to the pile settlements coupled with the relevant pile resistances (Figure 11). The comparison of the intersection of pile and soil settlements and load-resistance equilibria predicts the neutral plane at 3.1 m under the pile head, the load increment of 313 kN, and the pile head settlement of 27.7 mm.

Figure 11 further shows that a simplified approach, considering the neutral plane at the interface of consolidating and stable layers, would predict the total loading force, which mostly the pile base would have to carry, to be over 3 500 kN. Considering the initial pile settlement unaffected by negative skin friction would reduce the neutral plane position to approximately 12 m depth below the pile head with a loading force of 3 000 kN.

Let us check the results again with the refined approach using the nonlinear load-settlement curve construction (Figure 12). The comparison shows that the skin friction is not fully mobilised in the first five metres of sand from the pile head. The neutral plane, corresponding to the position where the negative skin friction switches to the positive one, is predicted at a depth of 3 m. The increase in the total loading force due to the down drag load is 179 kN, and the predicted settlement of 27.4 mm is again in good agreement with the previous practical analysis.

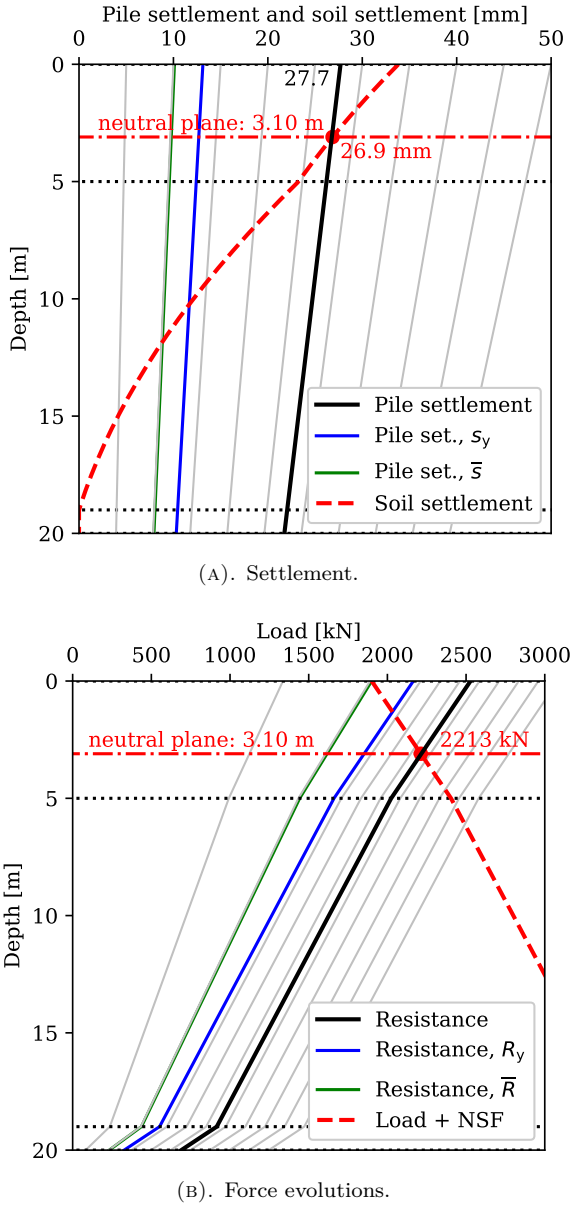

(A). Settlement.

(B). Force evolutions.

FIGURE 11. Example 2 – Settlement and force evolutions including negative skin friction (NSF) effect along the pile length provided by the practical approach [59]; (colour online).

5. CONCLUSION

This study compared two approaches:

(1.) a practical design framework for piles subjected to negative skin friction combining the load-settlement curve approximation proposed by Masopust with the Fellenius unified pile design concept,

(2.) a refined approach relating the mobilised skin friction directly to movements of individual pile segments and providing a nonlinear relationship between the pile head settlement and pile resistance.

The main conclusions from this study are:

- The surrounding soil settlements resulting in negative skin friction and drag force can significantly increase the pile settlement.

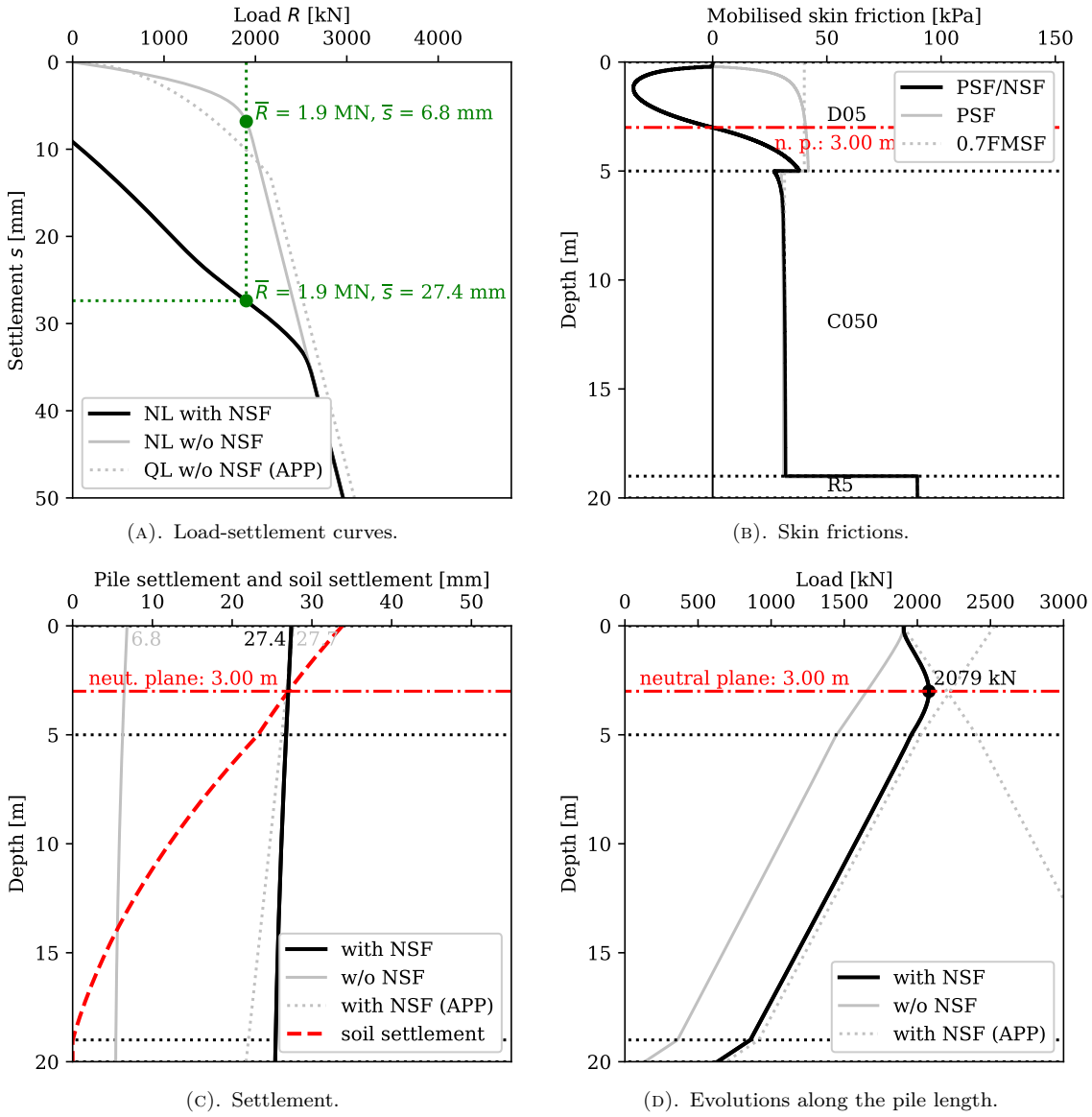

(A). Load-settlement curves.

(B). Skin frictions.

(C). Settlement.

(D). Evolutions along the pile length.

Figure 12. Example 2 – Comparison of the load-settlement curves, skin frictions (negative (NSF), positive (PSF), or 70 % fully mobilised (0.7FMSF)), and settlement and load evolutions along the pile length by nonlinear approach (NL) or practical approximation (APP) using quadratic-linear (QL) load-settlement curve; (colour online).

- The simplified approach, mentioned in the second generation of EC7, estimating the neutral plane at the boundary of the settling and stable layer, leads to an uneconomical pile design for ground profiles with a significant thickness of the compressible layer(s).
- The examples presented show a very good agreement between the practical approach based on the load-settlement approximation and the response of the refined model.

Let us point out that the used friction-settlements relationships from [55] or Appendix A may be further updated using load-transfer functions introduced in the proposed European standard [43] or the recent literature [42, 44, 62].

The next logical step would be to validate the model against experimental measurements. Unfortunately, a field measurement is beyond the scope of the grant projects that supported this research.

Acknowledgements

The financial support from the Czech Grant Agency, project No. 22-12178S, and by the Czech Technical University in Prague, within the project SGS23/040/OHK1/1T/11, is gratefully acknowledged.

References

[1] H. G. Poulos. Tall building foundations: Design methods and applications. *Innovative Infrastructure Solutions* **1**(1):10, 2016. https://doi.org/10.1007/s41062-016-0010-2

[2] H. G. Poulos, A. J. Davids. Foundation design for the emirates twin towers, dubai. *Canadian Geotechnical Journal* **42**(3):716–730, 2005. https://doi.org/10.1139/t05-004

[3] W. F. Baker, C. Brown, J. J. Pawlikowski, D. S. Rankin. Tall buildings and their foundations: Three examples. In *Proceedings of the 7th International Conference on Case Histories in Geotechnical Engineering*, pp. 1–10. Missouri University of Science and Technology, 2013.

[4] T. J. Ingham, S. Rodriguez, R. Donikian, J. Chan. Seismic analysis of bridges with pile foundations. *Computers & Structures* **72**(1–3):49–62, 1999. https://doi.org/10.1016/S0045-7949(99)00021-8

[5] H. Matlock, L. C. Reese. Foundation analysis of offshore pile supported structures. In *Proceedings of the 5th International Conference on Soil Mechanics and Foundation Engineering*, pp. 91–97. 1961.

[6] B. H. Fellenius. *Basics of foundation design: Electronic edition.* 2023. [2025-01-02]. https://www.fellenius.net/papers/444_The_Red_Book-Basics_of_Foundation_Design_2025.pdf

[7] A. Plomp, W. C. v. Mierlo. Special problems, effects of drainage by well points on pile foundations. In *Proceedings of 2nd International Conference on Soil Mechanics and Foundation Engineering*, vol. 4, pp. 141–148. 1948.

[8] I. J. Johannessen, L. Bjerrum. Measurement of the compression of a steel pile to rock due to settlement of the surrounding clay. In *6th International Conference on Soil Mechanics and Foundation Engineering*, pp. 261–264. 1965.

[9] M. A. Endo, A. Minou, I. Kawasaki, T. Shibata. Negative skin friction acting on steel pipe pile in clay. In *Proceedings of 7th International Conference on Soil Mechanics and Foundation Engineering*, pp. 85–92. 1969.

[10] B. H. Fellenius, B. B. Broms. Negative skin friction for long piles driven in clay. In *Proceedings of 7th International Conference on Soil Mechanics and Foundation Engineering*, vol. 2, pp. 93–98. 1969.

[11] B. H. Fellenius. Down-drag on piles in clay due to negative skin friction. *Canadian Geotechnical Journal* **9**(4):323–337, 1972. https://doi.org/10.1139/t72-037

[12] L. Bjerrum, I. J. Johannessen, O. Eide. Reduction of negative skin friction on steel piles to rock. In *Proceedings of 7th International Conference on Soil Mechanics and Foundation Engineering*, pp. 27–34. 1969.

[13] L. K. Walker, P. P. Le Darvall. Dragdown on coated and uncoated piles. In *Proceedings of 8th International Conference on Soil Mechanics and Foundation Engineering*, vol. 2, pp. 257–262. 1973.

[14] B. H. Fellenius. Downdrag on bitumen coated piles. *Journal of the Geotechnical Engineering Division* **105**(10):1262–1265, 1979.

[15] F. M. Clemente. Downdrag on bitumen coated piles in a warm climate. In *Proceedings of the 10th International Conference on Soil Mechanics and Foundation Engineering*, vol. 2, pp. 673–676. 1981.

[16] T. Shibata, H. Sekiguchi, H. Yukitomo. Model test and analysis of negative friction acting on piles. *Soils and Foundations* **22**(2):29–39, 1982. https://doi.org/10.3208/sandf1972.22.2_29

[17] B. Indraratna, A. S. Balasubramaniam, P. Phamvan, Y. K. Wong. Development of negative skin friction on driven piles in soft Bangkok clay. *Canadian Geotechnical Journal* **29**(3):393–404, 1992. https://doi.org/10.1139/t92-044

[18] J. Thomas, M. Fahey, R. Jewell. Pile down-drag due to surface loading. In *Centrifuge 98*, pp. 507–512. CRC Press, 1998.

[19] K. Tomisawa, J. Nishikawa. An evaluation of negative skin friction occurring on a pile foundation. In *ISRM International Symposium*, pp. ISRM–IS–2000–382. 2000.

[20] C. F. Leung, B. K. Liao, Y. K. Chow, et al. Behavior of pile subject to negative skin friction and axial load. *Soils and Foundations* **44**(6):17–26, 2004. https://doi.org/10.3208/sandf.44.6_17

[21] C. W. W. Ng, H. G. Poulos, V. S. H. Chan, et al. Effects of tip location and shielding on piles in consolidating ground. *Journal of Geotechnical and Geoenvironmental Engineering* **134**(9):1245–1260, 2008. https://doi.org/10.1061/(ASCE)1090-0241(2008)134:9(1245)

[22] S. Y. Lam, C. W. W. Ng, C. F. Leung, S. H. Chan. Centrifuge and numerical modeling of axial load effects on piles in consolidating ground. *Canadian Geotechnical Journal* **46**(1):10–24, 2009. https://doi.org/10.1139/T08-095

[23] Z. Zhao, S. Ye, Y. Zhu, et al. Scale model test study on negative skin friction of piles considering the collapsibility of loess. *Acta Geotechnica* **17**(2):601–611, 2022. https://doi.org/10.1007/s11440-021-01254-1

[24] Y. Hong, C. W. W. Ng, Y. M. Chen, et al. Field study of downdrag and dragload of bored piles in consolidating ground. *Journal of Performance of Constructed Facilities* **30**(3):04015050, 2016. https://doi.org/10.1061/(ASCE)CF.1943-5509.0000790

[25] L. Zeevaert. Reduction of point bearing capacity of piles because of negative friction. In *Proceedings of the First Pan-American Conference on Soil Mechanics and Foundation Engineering*, pp. 1145–1151. 1959.

[26] E. M. Comodromos, S. V. Bareka. Evaluation of negative skin friction effects in pile foundations using 3D nonlinear analysis. *Computers and Geotechnics* **32**(3):210–221, 2005. https://doi.org/10.1016/j.compgeo.2005.01.006

[27] B. H. Fellenius. Negative skin friction and settlement of piles. In *Proceedings of the Second International Seminar, Pile Foundations*, pp. 1–12. Nanyang Technological Institute, 1984.

[28] B. H. Fellenius. Unified design of piles and pile groups. *Transportation Research Record* **1169**:75–82, 1988.

[29] H. G. Poulos, N. S. Mattes. The analysis of downdrag in end-bearing piles. In *Proceedings of 7th International Conference on Soil Mechanics and Foundation Engineering*, pp. 203–209. 1969.

[30] R. D. Mindlin. Force at a point in the interior of a semi-infinite solid. *Physics* **7**(5):195–202, 1936. https://doi.org/10.1063/1.1745385

[31] H. G. Poulos, E. H. Davis, et al. *Pile foundation analysis and design*, vol. 397. Wiley New York, USA, 1980.

[32] H. G. Poulos. Piles subjected to negative friction: A procedure for design. *Geotechnical Engineering* **28**:23–44, 1997.

[33] H. G. Poulos. A practical design approach for piles with negative friction. *Proceedings of the Institution of Civil Engineers-Geotechnical Engineering* **161**(1):19–27, 2008. https://doi.org/10.1680/geng.2008.161.1.19

[34] H. M. Coyle, L. C. Reese. Load transfer for axially loaded piles in clay. *Journal of the Soil Mechanics and Foundations Division* **92**(2):1–26, 1966. https://doi.org/10.1061/JSFEAQ.0000850

[35] M. F. Randolph, C. P. Wroth. Analysis of deformation of vertically loaded piles. *Journal of the Geotechnical Engineering Division* **104**(12):1465–1488, 1978. https://doi.org/10.1061/AJGEB6.0000729

[36] E. E. Alonso, A. Josa, A. Ledesma. Negative skin friction on piles: A simplified analysis and prediction procedure. *Géotechnique* **34**(3):341–357, 1984. https://doi.org/10.1680/geot.1984.34.3.341

[37] K. S. Wong, C. I. Teh. Negative skin friction on piles in layered soil deposits. *Journal of Geotechnical Engineering* **121**(6):457–465, 1995. https://doi.org/10.1061/(ASCE)0733-9410(1995)121:6(457)

[38] C. I. Teh, K. S. Wong. Analysis of downdrag on pile groups. *Géotechnique* **45**(2):191–207, 1995. https://doi.org/10.1680/geot.1995.45.2.191

[39] W. D. Guo, M. F. Randolph. Rationality of load transfer approach for pile analysis. *Computers and Geotechnics* **23**(1–2):85–112, 1998. https://doi.org/10.1016/S0266-352X(98)00010-X

[40] M. Sutman, C. G. Olgun, L. Laloui. Cyclic load – transfer approach for the analysis of energy piles. *Journal of Geotechnical and Geoenvironmental Engineering* **145**(1):04018101, 2019. https://doi.org/10.1061/(ASCE)GT.1943-5606.0001992

[41] H. Song, H. Pei, J.-M. Pereira, et al. A simple load transfer method for energy pile groups. *Computers and Geotechnics* **159**:105483, 2023. https://doi.org/10.1016/j.compgeo.2023.105483

[42] W. Wu, Z. Wang, Y. Zhang, et al. Semi-analytical solution for negative skin friction development on deep foundations in coastal reclamation areas. *International Journal of Mechanical Sciences* **241**:107981, 2023. https://doi.org/10.1016/j.ijmecsci.2022.107981

[43] CEN/TC 250 SC7 European Committee for Standardization. prEN 1997-3. Eurocode 7: Geotechnical design – Part 3: Geotechnical structures, 2022.

[44] W. Cao, Y. Chen, W. E. Wolfe. New load transfer hyperbolic model for pile-soil interface and negative skin friction on single piles embedded in soft soils. *International Journal of Geomechanics* **14**(1):92–100, 2014. https://doi.org/10.1061/(ASCE)GM.1943-5622.0000289

[45] R. P. Chen, W. H. Zhou, Y. M. Chen. Influences of soil consolidation and pile load on the development of negative skin friction of a pile. *Computers and Geotechnics* **36**(8):1265–1271, 2009. https://doi.org/10.1016/j.compgeo.2009.05.011

[46] H.-J. Kim, J. L. C. Mission. Development of negative skin friction on single piles: Uncoupled analysis based on nonlinear consolidation theory with finite strain and the load-transfer method. *Canadian Geotechnical Journal* **48**(6):905–914, 2011. https://doi.org/10.1139/t11-004

[47] J. Liu, H. Gao, H. Liu. Finite element analyses of negative skin friction on a single pile. *Acta Geotechnica* **7**(3):239–252, 2012. https://doi.org/10.1007/s11440-012-0163-x

[48] S. Jeong, J. Lee, C. J. Lee. Slip effect at the pile–soil interface on dragload. *Computers and Geotechnics* **31**(2):115–126, 2004. https://doi.org/10.1016/j.compgeo.2004.01.009

[49] P.-T. Simic-Silva, B. Martínez-Bacas, R. Galindo-Aires, D. Simic. 3D simulation for tunnelling effects on existing piles. *Computers and Geotechnics* **124**:103625, 2020. https://doi.org/10.1016/j.compgeo.2020.103625

[50] J.-S. Chiou, W.-T. Wei. Numerical investigation of pile-head load effects on the negative skin friction development of a single pile in consolidating ground. *Acta Geotechnica* **16**(6):1867–1878, 2021. https://doi.org/10.1007/s11440-020-01134-0

[51] R. Liang, Z.-Y. Yin, J.-H. Yin, P.-C. Wu. Numerical analysis of time-dependent negative skin friction on pile in soft soils. *Computers and Geotechnics* **155**:105218, 2023. https://doi.org/10.1016/j.compgeo.2022.105218

[52] CEN/TC 250 European Committee for Standardization. EN 1997-1. Eurocode 7: Geotechnical design – Part 1: General rules, 2004.

[53] R. Driscoll, B. Simpson. EN1997 Eurocode 7: Geotechnical design. *Proceedings of the Institution of Civil Engineers-Civil Engineering* **144**(6):49–54, 2001. https://doi.org/10.1680/cien.2001.144.6.49

[54] S. A. Tan, B. H. Fellenius. Negative skin friction pile concepts with soil–structure interaction. *Geotechnical Research* **3**(4):137–147, 2016. https://doi.org/10.1680/jgere.16.00006

[55] J. Masopust. *Vrtané piloty [In Czech; Bored piles].* Čeněk a Ježek s.r.o., 1994.

[56] Z. Bazant, J. Masopust. Drilled pier design based on load-settlement curve. In *Proceedings of the 10^{th} International Conference on Soil Mechanics and Foundation Engineering*, vol. 2, pp. 615–618. 1981.

[57] J. Masopust. Design of axially loaded bored single piles. In *Proceedings of the 4^{th} International Seminar on Deep Foundations on Bored and Auger Piles*, pp. 203–208. 2003.

[58] J. Masopust. Design of axially loaded bored single piles in the Czech Republic. In *Proceedings of the International Conference on Case Histories in Geotechnical Engineering*. University of Missouri – Rolla, 2004. [2025-01-02]. https://scholarsmine.mst.edu/icchge/5icchge/session01/2

[59] Úřad pro technickou normalizaci, metrologii a státní zkušebnictví. ČSN 73 1004. Navrhování základových konstrukcí – Stanovení požadavků pro výpočetní metody [In Czech; Geotechnical design – Foundations – Requirements for calculation methods], 2020.

[60] V. Anderle, A. Zemanová, J. Masopust. Zohlednění vlivu negativního plášťového tření při výpočtu sedání pilot metodou regresních součinitelů [In Czech; Consideration of the effect of negative skin friction in the calculation of pile settlement by the method of regression coefficients]. In *Sborník 51. konference Zakládání staveb Brno 2023*, pp. 133–140. 2023.

[61] A. Zemanová. Piles with NSF – supplementary code for results presented, 2023. [2023-12-22]. `https://gitlab.com/zemanova.alena/piles-with-nsf`

[62] L. Li, J. Li, Y. Wang, W. Gong. Analysis of nonlinear load-displacement behaviour of pile groups in clay considering installation effects. *Soils and Foundations* **60**(4):752–766, 2020. `https://doi.org/10.1016/j.sandf.2020.04.008`

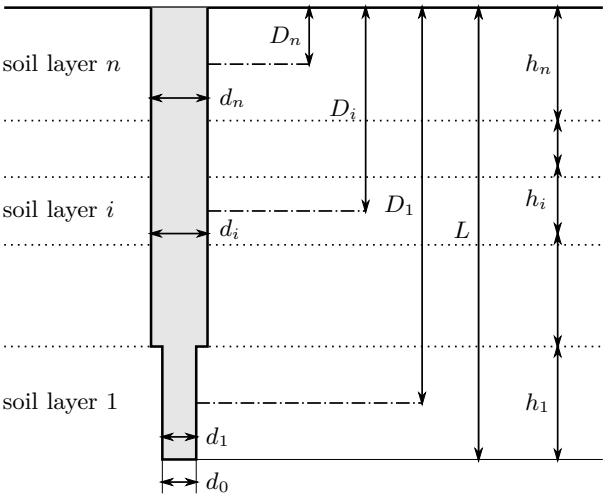

Figure 13. Pile in a layered soil deposit

Appendix A.

A.1. Practical approach providing a quadratic-linear approximation of the load-settlement curve

The load-settlement curve is approximated by a parabola continued by a straight line [55–58] and Figure 2. The coordinates of two points corresponding to the full mobilisation of skin friction (s_y; R_y) and to the axial load-bearing capacity at the 25 mm settlement ($s_{25} = 25\,\mathrm{mm}$; R_{25}) are necessary to construct the load-settlement curve.

The values of settlement and loading force corresponding to the full mobilisation of skin friction (s_y; R_y) determine the first branch of the parabola-shaped curve for the load-interval $R \in \langle 0, R_\mathrm{y}\rangle$:

$$s = s_\mathrm{y}\left(\frac{R}{R_\mathrm{y}}\right)^2. \tag{1}$$

In the interval starting at the full mobilisation point and ending at the load-bearing capacity of pile corresponding to the 25 mm settlement $R \in \langle R_\mathrm{y}, R_{25}\rangle$, the second branch of the load-settlement curve is given by the straight line with the coordinates of the endpoint ($s_{25} = 25\,\mathrm{mm}$; R_{25}):

$$s = s_\mathrm{y} + (s_{25} - s_\mathrm{y})\frac{R - R_\mathrm{y}}{R_{25} - R_\mathrm{y}}. \tag{2}$$

Thus, the increase in shaft resistance is assumed to be quadratic whereas the base resistance is supposed to be linearly related to the pile head settlement.

Taking into account the notation for a single pile geometry in a layered soil deposit in Figure 13, the relations for determining all quantities needed for the load-settlement curve construction, i.e., the pile settlement corresponding to the full mobilisation of skin friction s_y, the pile load corresponding to the full mobilisation of skin friction R_y, and the load-bearing capacity of the pile R_{25}, are given by equations below. The value of the axial load-bearing capacity of the pile R_{25} consists of the shaft and base resistance, R_sy and $R_{\mathrm{b},25}$:

$$R_{25} = R_\mathrm{sy} + R_{\mathrm{b},25}. \tag{3}$$

The pile is divided into several parts corresponding to the independent soil layers (Figure 13), and then, the fully mobilised load-bearing capacity of the pile shaft is given by combining skin friction contributions from the soil layers:

$$R_\mathrm{sy} = 0.7m\pi\sum_{i=1}^{n} d_i h_i q_{si}, \tag{4}$$

where the coefficient reflecting the effect of the pile shaft surface m is given in Table 2 and the diameters of pile segments in the i-th layer d_i and the thicknesses of soil in the i-th layer h_i are set according to Figure 13. Back analysis of static load tests on single bored piles provided a set of load-settlements curves, from which the

Value	Methods of pile installation and insulation
1.0	Unsupported excavations, concreting in a dry borehole or under the water level
0.9	Excavations under excavation-support fluids
0.7	Piles with secondary shaft insulation made of PVC or PE foils with thickness > 0.7 mm
0.5	Piles with secondary shaft insulation made of PVC foil and wire netting,
0.15	Piles with the permanent casting of steel tubes

TABLE 2. Installation coefficient reflecting the effect of the pile shaft surface m.

Rock/Soil	a	b	e	f
Weak rocks with uniaxial compressive strength of 15–20 MPa (R3)	246	226	2841	1299
Weak rocks with uniaxial compressive strength of 5–15 MPa (R4)	170	139	1616	1155
Weak rocks with uniaxial compressive strength of 1.5–5 MPa (R5)	132	95	958	704
Cohesionless soils with density index $I_D = 0.9$ (D9)	154	116	1597	1399
Cohesionless soils with density index $I_D = 0.7$ (D7)	91	48	490	445
Cohesionless soils with density index $I_D = 0.5$ (D5)	62	16	268	175
Cohesive soils with consistency index $I_C \geq 1.0$ (C100)	97	109	988	1084
Cohesive soils with consistency index $I_C = 0.75$ (C075)	71	65	593	617
Cohesive soils with consistency index $I_C = 0.5$ (C050)	46	21	198	150

TABLE 3. Regression coefficients a, b, c, and d [kPa] for various rocks and soils.

relationships for the ultimate shaft frictions q_{si} and the base resistance corresponding to the full mobilisation of the shaft friction were derived. Thus, the limit shaft friction in the i-th layer is provided by a hyperbolic law:

$$q_{si} = a - \frac{b}{\left(\frac{D_i}{d_i}\right)}, \tag{5}$$

and the base resistance q_0 corresponding to the full mobilisation of the shaft friction is described likewise:

$$q_0 = e - \frac{f}{\left(\frac{L}{d_0}\right)}, \tag{6}$$

using the couples of regression coefficients a, b and e, f according to Table 3 and slenderness ratios derived from the distance of the pile cap and the middle of the i-th layer D_i, the pile length L, and the diameters of pile shaft d_i or base d_0 (Figure 13).

Due to the layered soil profile, the weighted average of skin frictions along the pile shaft may be determined as:

$$q_s = \frac{\sum_{i=1}^{n} d_i h_i q_{si}}{\sum_{i=1}^{n} d_i h_i}. \tag{7}$$

The base capacity corresponding to the 25 mm pile settlement, assuming its linear increase in depth, is given by:

$$R_{b,25} = \beta R_y \frac{s_{25}}{s_y}, \tag{8}$$

employing the coefficient of load transfer to the pile base:

$$\beta = \frac{q_0}{q_0 + 4q_s \frac{L}{d_0}}. \tag{9}$$

Thus, the pile load corresponding to the full mobilisation of the shaft friction may be expressed according to Poulos's method [31] as:

$$R_y = \frac{R_{sy}}{1 - \beta}. \tag{10}$$

Finally, the pile settlement corresponding to the full mobilisation of skin friction is determined following [31] as:

$$s_y = I \frac{R_y}{dE_s}, \tag{11}$$

Layer thickness	Moduli for given pile diameter and weak rock type [MPa]								
h	$d = 0.6$ m			$d = 1.0$ m			$d = 1.5$ m		
[m]	R3	R4	R5	R3	R4	R5	R3	R4	R5
1.5	50.3	28.2	20.0	72.3	35.0	24.7	85.5	33.5	22.3
3	64.5	43.1	30.8	106	57.3	41.0	138	58.8	41.2
5		58.2	41.3		75.3	54.8		87.9	63.7
10		87.5	61.6		115	83.2		133	97.0

TABLE 4. Secant deformation moduli E_s [MPa] for piles in weak rocks.

Layer thickness	Moduli for given pile diameter and cohesionless soil type [MPa]								
h	$d = 0.6$ m			$d = 1.0$ m			$d = 1.5$ m		
[m]	$I_D = 0.5$	0.7	0.9	$I_D = 0.5$	0.7	0.9	$I_D = 0.5$	0.7	0.9
1.5	11.0	13.7	28.3	12.8	15.8	30.6	13.0	15.3	29.0
3	15.5	20.2	44.5	18.4	25.0	47.8	19.4	24.5	52.5
5	18.8	26.6	56.1	22.8	32.5	69.1	24.5	36.0	78.2
10	23.8	36.6	72.1	29.8	47.8	93.4	32.6	54.0	107

TABLE 5. Secant deformation moduli E_s [MPa] for piles in cohesionless soils.

Layer thickness	Moduli for given pile diameter and cohesive soil type [MPa]								
h	$d = 0.6$ m			$d = 1.0$ m			$d = 1.5$ m		
[m]	$I_C = 0.5$	0.75	≥ 1	$I_C = 0.5$	0.75	≥ 1	$I_C = 0.5$	0.75	≥ 1
1.5	6.9	10.0	13.2	7.9	10.7	13.4	8.6	10.5	12.3
3	10.0	15.5	22.0	12.5	18.6	23.9	13.7	18.4	23.0
5	12.5	21.9	31.2	15.9	25.7	33.4	18.4	27.6	36.7
10	15.5	29.9	44.3	21.3	36.3	51.3	24.6	41.0	57.4

TABLE 6. Secant deformation moduli E_s [MPa] for piles in cohesive soils.

with the influence factor of pile settlement:

$$I = I_1 R_\mathrm{k}, \tag{12}$$

consisting of the basic influence factor I_1 multiplied by the correction factor R_k representing the effect of the pile stiffness $K = \frac{E_\mathrm{pile}}{E_\mathrm{s}}$ and slenderness $\frac{L}{d}$ may be derived from plots presented in [31] or [55].

For layered soil deposits, the secant deformation modulus along the pile shaft is replaced by its weighted average:

$$E_\mathrm{s} = \frac{\sum_{i=1}^{n} E_{\mathrm{s}i} h_i}{\sum_{i=1}^{n} h_i}, \tag{13}$$

using the moduli for individual soil layers in Tables 4, 5, and 6 determined from the back analysis of static loading tests.

A.2. Refined approach providing a nonlinear load-settlement curve

The nonlinear load-settlement curve is constructed according to the procedure outlined in Figure 14. First, the pile length is divided into N elements (Figure 5), and a small vertical displacement (settlement s_0) is assigned to the pile base. Then, the pile base resistance q_0 caused by its movement s_0 is derived from a transfer function. For the purpose of this study, which focuses on negative skin friction, we adjusted this relationship to achieve the same pile resistance as in the previous practical approach because we wanted to separate the errors resulting from a different approximation of the base response. Then, the resultant force acting on the pile base with its cross-sectional area A_0 follows as $R_0 = q_0 A_0$.

For the shaft, we employed the load transfer functions motivated by Ménard's rheological model, described in [55]. Then, the shaft friction for the i-th element $q_{\mathrm{s}i}$ is supposed to be related to the vertical movement of

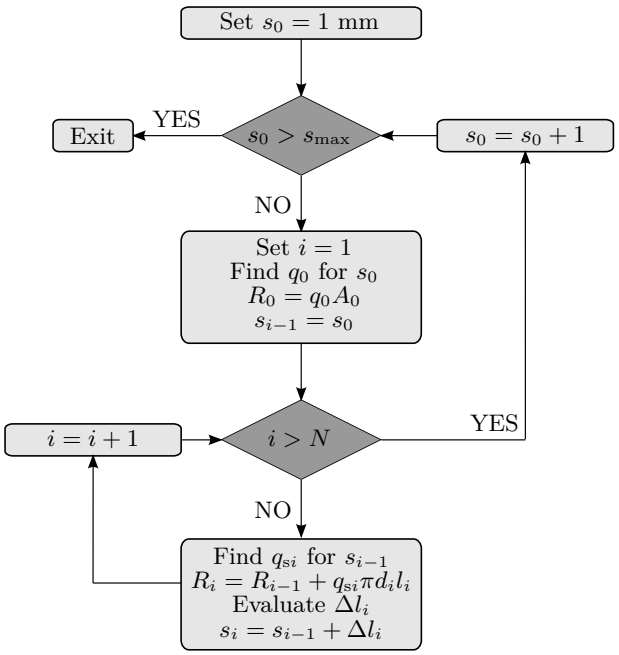

FIGURE 14. Flowchart of the algorithm providing the nonlinear load-settlement curve.

Rock/Soil	$\boldsymbol{\alpha_i}$	$\boldsymbol{f_i}$	$\boldsymbol{E_{\mathrm{p},i}}$ **[kPa]**
Weak rocks with uniaxial compressive strength of 15–20 MPa (R3)	0.66	3.02	80
Weak rocks with uniaxial compressive strength of 5–15 MPa (R4)	0.66	3.02	50
Weak rocks with uniaxial compressive strength of 1.5–5 MPa (R5)	0.66	3.02	30
Cohesionless soils with density index $I_{\mathrm{D}} = 0.9$ (D9)	0.66	3.02	40
Cohesionless soils with density index $I_{\mathrm{D}} = 0.7$ (D7)	0.66	3.02	20
Cohesionless soils with density index $I_{\mathrm{D}} = 0.5$ (D5)	0.66	3.02	10
Cohesive soils with consistency index $I_{\mathrm{C}} \geq 1.0$ (C100)	0.5	4.50	25
Cohesive soils with consistency index $I_{\mathrm{C}} = 0.75$ (C075)	0.5	4.50	15
Cohesive soils with consistency index $I_{\mathrm{C}} = 0.5$ (C050)	0.5	4.50	8

TABLE 7. Parameters α_i f_i, and pressiometric moduli $E_{\mathrm{p},i}$ for various rocks and soils.

the element $s_{(i-1)}$ (see Figure 5) by:

$$q_{\mathrm{s}i} = 0.7 m q_{\mathrm{s,lim},i} \left(1 - \left(1 - \frac{s_{(i-1)}}{s_{\mathrm{s,lim},i}}\right)^{f_i}\right). \tag{14}$$

Here, the parameter m follows again from Table 2, the limit skin friction $q_{\mathrm{s,lim},i}$ is derived from the regression values following the previous approach, and the corresponding pile head settlement is assumed to be:

$$s_{\mathrm{s,lim},i} = 0.7 \frac{q_{\mathrm{s,lim},i}}{E_{\mathrm{p}}} g_i(\alpha_i, d). \tag{15}$$

Other required parameters for the approximation of the skin friction mobilisation are listed for different types of rocks and soils in Table 7 and complemented with the function $g(\alpha_i, d_i)$ (Table 8).

Due to the fine division of the pile into individual parts, we assume that the average vertical movement of the element s_{i-1} corresponds simply to the vertical settlement of its bottom plane. Then, the force acting on the top cross-section (Figure 5) holds:

$$R_i = R_{i-1} + q_{\mathrm{s}i}\pi d_i l_i. \tag{16}$$

Using the elastic contraction of the element length:

$$\Delta l_i = \frac{(R_i + R_{i+1}) l_i}{2 E_{\mathrm{pile}} A_i}, \tag{17}$$

Diameter $\boldsymbol{d_i}$ **[m]**	$\boldsymbol{\alpha_i} = 0.5$	$\boldsymbol{\alpha_i} = 0.66$
0.6	2.997	1.892
0.8	3.460	2.287
1.0	3.869	2.650
1.2	4.238	2.989
1.4	4.577	3.309
1.6	4.893	3.614
1.8	5.190	3.906
2.0	5.471	4.188

TABLE 8. Values of function g_i for different pile diameters d_i and rheological coefficients α_i.

the settlement of the element top is written as:

$$s_i = s_{i-1} + \Delta l_i. \tag{18}$$

In this way, one proceeds to the pile head, where its settlement is derived. The force at the pile head R_N corresponds to the pile resistance for the given base and head settlement s_0 and s_N.

Repeating this procedure for gradually increasing base settlement (Figure 14) provides couples of pile head forces and settlements that can be plotted, providing the nonlinear load-settlement curve.